NANO LETTERS

LETTER

pubs.acs.org/NanoLett

Sequential Cation Exchange in Nanocrystals: Preservation of Crystal Phase and Formation of Metastable Phases

Hongbo Li,[†] Marco Zanella,[†] Alessandro Genovese,[†] Mauro Povia,[†] Andrea Falqui,[†] Cinzia Giannini,[‡] and Liberato Manna*[,†]

[†]Istituto Italiano di Tecnologia, via Morego 30, 16163 Genova, Italy

[‡]CNR-Istituto di Crystallografia (IC), Via Amendola 122/O, I-70126 Bari, Italy

Supporting Information

ABSTRACT: We demonstrate that it is possible to convert CdSe nanocrystals of a given size, shape (either spherical or rod shaped), and crystal structure (either hexagonal wurtzite, i.e., hexagonal close packed (hcp), or cubic sphalerite, i.e., face-centered cubic (fcc)), into ZnSe nanocrystals that preserve all these characteristics of the starting particles (i.e., size, shape, and crystal structure), via a sequence of two cation exchange reactions, namely, $Cd^{2+} \Rightarrow Cu^{+} \Rightarrow Zn^{2+}$. When starting from hexagonal wurtzite CdSe nanocrystals, the exchange of Cd^{2+} with Cu^{+} yields Cu_2Se nanocrystals in a metastable hexagonal phase, of which we could follow the transformation to the more stable fcc phase for a single nanorod, under the electron microscope. Remarkably, these metastable hcp Cu_2Se nanocrystals can be converted in solution into ZnSe nanocrystals, which yields ZnSe nanocrystals in a pure hcp phase.

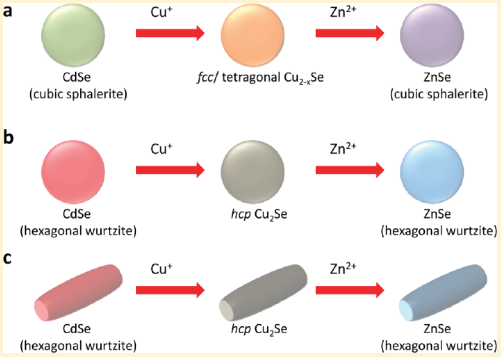

KEYWORDS: Cation exchange, nanocrystals, copper selenide, ZnSe, metastable phases, semiconductors

The synthesis and the study of physical properties of colloidal inorganic nanocrystals (NCs) with controlled size, shape, and crystal phase are active areas of research in nanoscience.[1,2] Developments include the ability to synthesize NCs with sections/shells made of different materials, which extends their range of applications.[3−6] A recent toolkit available for the synthesis of NCs is represented by cation exchange reactions, by which the sublattice of cations in ionic NCs can be replaced with a new sublattice of other cations preserving the characteristic of the crystallographic sites involved in ion substitution, while the sublattice of anions remains in place,[7−10] which yields NCs of a new material but preserves the size and the shape of the starting NCs. Therefore, cation exchange reactions provide a pathway to design novel NCs with specific morphology and sometimes even a specific crystal phase, starting from a generation of well-developed NCs (for instance NCs of cadmium chalcogenides). Novel heterostructures have been shown to form via partial cation exchange, due to minimization of lattice strain,[8] or nanorods were made via sequential cation exchange reactions,[11] and various NC morphologies and compositions were obtained when combining this technique with other synthesis tools.[12,13] One key aspect of these reactions, as highlighted above, is that the anion sublattice is maintained.[9] Also, in some cases cation exchange has been shown to yield metastable phases in nanocrystals. Pietryga et al. for example have demonstrated that it is possible to get metastable rock salt CdSe (which would be stable only at high pressure) by partial cation exchange of rock salt PbSe.[14] In that case the formation of CdSe rock salt phase minimized the strain at the PbSe−CdSe interface. As another example, Luther et al. obtained Cu_2S in metastable low chalcocite phase by cation exchange of CdS NCs.[11]

Here we demonstrate that it is possible to convert CdSe NCs of a given size, shape (either spherical or rod-shaped), and crystal structure (either hexagonal wurtzite, i.e., hexagonal close packed (hcp), or cubic sphalerite, i.e., face-centered cubic (fcc)), into ZnSe NCs that preserve all these characteristics of the starting particles, via a sequence of two cation exchange steps, namely, $Cd^{2+} \Rightarrow Cu^{+} \Rightarrow Zn^{2+}$ (see Scheme 1). Hence, the intermediate copper selenide NCs were able to transfer all the morphological and structural information of CdSe to ZnSe. The three remarkable points of the work are as follows:

(i) As was well established in previous reports by several groups, no direct displacement of Cd^{2+} by Zn^{2+} has been found to be possible on CdSe NCs: the Zn^{2+} ions appear unable to displace the Cd^{2+} ions, while they can absorb on the surface of the CdSe NCs, and this is at the base of the formation of core/shell NCs. This is clear from several works on the synthesis the core/shell CdSe/ZnS NCs[15,16] and CdSe/ZnSe NCs.[17,18] Therefore, only a sequence of two exchange steps could ultimately achieve exchange of Cd^{2+} with Zn^{2+}, as we show here. Furthermore, despite the $Cu^{+} \Rightarrow Zn^{2+}$ exchange at least in copper selenide was

Received: August 23, 2011
Revised: September 19, 2011
Published: September 30, 2011

Scheme 1. Various Cation Exchange Reactions Starting from CdSe NCs of a Given Size, Shape, and Crystal Phase Reported Here: (a) from Cubic Sphalerite (fcc) CdSe Spheres to Sphalerite (fcc) ZnSe Spheres through a Mixture of fcc and Tetragonal $Cu_{2-x}Se$ Spheres; (b) from hcp CdSe Spheres to hcp ZnSe Spheres through a Metastable hcp Cu_2Se Phase; (c) from hcp CdSe Nanorods to hcp ZnSe Nanorods, through Nanorods of the Same Metastable hcp Cu_2Se Phase

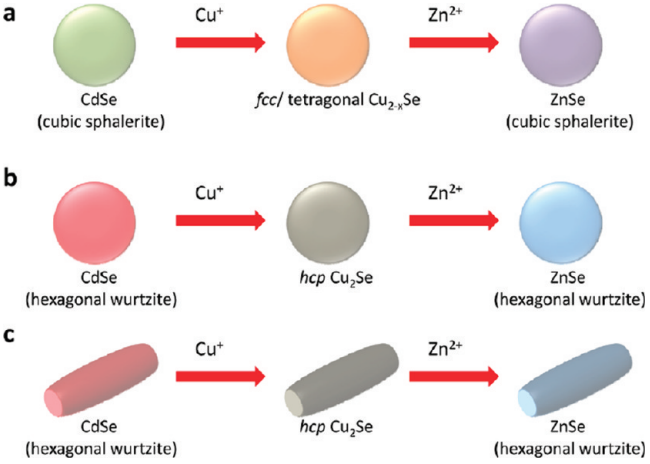

not documented so far, this transformation could be achieved by us under specific reaction conditions, most notably the use of trioctylphosphine (as a soft base to help the extraction of Cu^+ ions from the lattice) and of high reaction temperature.

(ii) When replacing Cd^{2+} with Cu^+ ions in hcp CdSe NCs, the sublattice of selenide ions remains in place, and therefore the resulting NCs too are in a hexagonal (hcp) crystalline phase. Also, these NCs were found to have a Cu:Se stoichiometry close to 2:1,[19] and not 1:1 as for the stable hexagonal phase of bulk copper selenide. They are therefore in a metastable hcp Cu_2Se phase, which has not been observed in the bulk so far but it was reported by Fenske et al.[20−23] only on molecular clusters. This phase could be identified by combining X-ray powder diffraction (XRD), including modeling of the XRD pattern, and transmission electron microscopy (TEM), the latter carried out at cryogenic temperature. Additionally, we could monitor in situ the transition from the metastable hcp phase to the fcc phase in a single Cu_2Se NC while this was observed under the electron beam of the TEM. Hence, the present work is yet another example of how cation exchange can be exploited to synthesize NCs in crystal phases that would be unstable in the bulk for a given material.

(iii) These metastable hcp Cu_2Se NCs can be converted into ZnSe NCs, which yields ZnSe NCs in a pure hcp phase. The hcp phase appears to be rare for ZnSe, since the more stable phase for this material is fcc,[24,25] and indeed only a few reports have demonstrated the successful synthesis of hcp ZnSe nanostructures at low temperature (compared to vapor phase approaches) up to now.[26−28] Furthermore, due to the relatively small difference in the total energy between the fcc and the hcp phases of ZnSe, the obtained samples of ZnSe NCs contained in reality a mixture of both phases.[24] Our work demonstrates instead a new route to pure colloidal hcp ZnSe NCs, with shape control in addition.

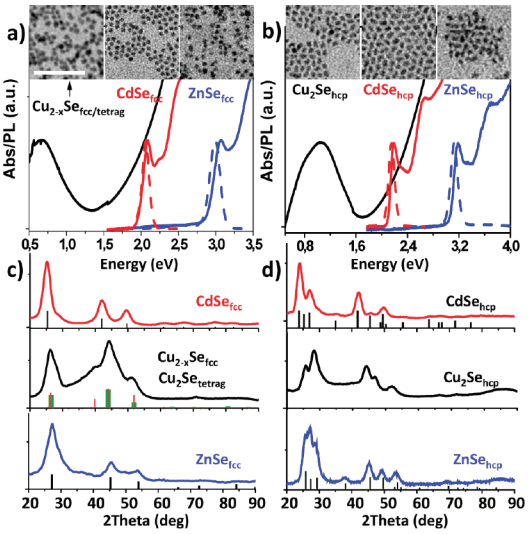

Figure 1. (a) Conventional TEM images and optical absorption/emission spectra of fcc/tetragonal $Cu_{2-x}Se$ spherical NCs (black line), *fcc* CdSe spherical NCs (red lines), and fcc ZnSe (blue lines) spherical NCs. (b) Conventional TEM images and optical absorption/emission spectra of hcp spherical Cu_2Se NCs (black line), hcp spherical CdSe NCs (red lines), and hcp ZnSe (blue lines) spherical NCs. The TEM images are all at the same magnification and the scale bar is 50 nm. (c, d) XRD patterns of the same samples as in (a) and (b), with black bars marking the bulk peak positions and intensities of fcc (c) and hcp (d) phases, except for the $Cu_{2-x}Se$ case (panel c, middle pattern), where the large green bars refer to fcc $Cu_{2-x}Se$ (berzelianite) and red bars refer to tetragonal Cu_2Se.

Our starting samples, all prepared according to literature protocols, were NCs of various sizes and shapes. We discuss here in detail the following representative samples: "spherical" fcc CdSe NCs of 3.2 ± 0.5 nm in size, "spherical" hcp CdSe NCs of 3.7 ± 0.7 nm in size, and rod-shaped hcp CdSe NCs of 6.6 ± 1.1 nm in diameter and 25.9 ± 2.6 nm in length. On all samples, exchange of Cd^{2+} with Cu^+ was carried out as described by Sadtler et al. for converting CdS NCs into Cu_2S NCs, i.e., using tetrakis(acetonitrile)copper(I) hexafluorophosphate as Cu(I) source dissolved in methanol, at room temperature, followed by standard purification procedures.[29] The copper selenide NCs were then subjected to exchange of Cu^+ with Zn^{2+}. This was done at temperatures ranging from 100 to 250 °C, using $ZnCl_2$ as zinc precursor, in a mixture of octadecene, oleylamine, and trioctylphosphine (TOP).[19]

In all the experiments it was straightforward to monitor the progress of the reaction, since the color changes in solution were obvious in both steps. In the $Cd^{2+} \Rightarrow Cu^+$ exchange step, the initial color of the solution (which ranged from yellow to dark red depending on the size of the CdSe NCs) turned into brown as soon as the copper precursor was added. In the $Cu^+ \Rightarrow Zn^{2+}$ exchange step, the brown color of the copper selenide NCs turned colorless or slightly yellow (again depending on the size of the ZnSe NCs) upon injection of the solution of NCs into the hot solution containing the Zn salt. For both steps, the reaction was completed in a few seconds, and the overall conversion of CdSe NCs to ZnSe NCs was quantitative, based on optical emission and absorption spectra on solutions of NCs and on elemental

dx.doi.org/10.1021/nl202927a |*Nano Lett.* 2011, 11, 4964–4970

analysis via inductively coupled plasma (ICP) optical emission spectroscopy on digested solutions.[19]

In the case of spherical fcc CdSe NCs, the sequence of exchange steps yielded spherical ZnSe NCs of the same size and of the fcc phase, as inferred by TEM (for size and shape) and by XRD; see Figure 1a,c. Also, the XRD pattern of the intermediate copper selenide NCs (always recorded by keeping the sample under vacuum to prevent oxidation)[19] could be indexed according to a mixture of fcc $Cu_{2-x}Se$ (matching the pattern of the berzelianite mineral) and tetragonal Cu_2Se (bellidoite) phases (also for bellidoite one cannot exclude a deviation from the 2:1 stoichiometry, as found for example by De Montreuil).[30] The cubic and tetragonal phases of $Cu_{2-x}Se$ are very similar to each other in terms of unit cells: the tetragonal cell can be seen as built from a 2 × 2 × 2 supercell of fcc cells and then slightly stretched along the *c* axis.[30,31] The broad peaks in XRD in this case could be ascribed to a combination of small scattering domains and disorder in the occupancies of the various possible sites for Cu(I) ions in the cubic and tetragonal lattices. It is worthy of note that also large (10−15 nm diameter) cubic berzelianite $Cu_{2-x}Se$ NCs, directly grown in solution according to previous works[12,13] (therefore not obtained by cation exchange from CdSe), were converted entirely into fcc ZnSe NCs if the same $Cu^+ \Rightarrow Zn^{2+}$ exchange procedure was followed, and the starting and final samples were practically indistinguishable from each other in terms of size and morphology under low-resolution TEM,[19] which confirms the validity and reproducibility of our $Cu^+ \Rightarrow Zn^{2+}$ exchange procedure. Optical absorption/emission spectra (Figure 1a) of the various NC samples (CdSe, intermediate $Cu_{2-x}Se$ and final ZnSe NCs), as well as elemental ICP analysis, indicated a quantitative CdSe ⇒ $Cu_{2-x}Se$ ⇒ ZnSe transformation. Also, the optical absorption spectrum of the copper selenide NCs evidenced a broad peak in the near-infrared (NIR) region. This peak is plasmonic in nature, as found by us in a previous work,[32] and is indicative of a Cu:Se stoichiometric ratio slightly below 2:1.

When starting instead from spherical hcp CdSe NCs, the same experiments yielded spherical hcp ZnSe NCs, as confirmed by TEM (for size and shape, see Figure 1b) and by XRD (Figure 1d), with again a quantitative conversion into ZnSe, as seen from the optical spectra (Figure 1b). In this case, however, the XRD pattern of the intermediate copper selenide NCs (Figure 1d) could not be indexed unambiguously according to any known phase of copper selenide. Elemental analysis of this sample (via ICP) gave a Cu:Se ratio close to 2:1.[19] Assessment of the chemical composition via ICP needed to be done carefully, since the excess unreacted Cu complex was difficult to separate quantitatively from the NCs in a single purification step, especially in samples of small (i.e., 3−4 nm diameter) nanoparticles. On the other hand, NC samples cleaned several times[19] had a Cu:Se ratio in the range 2.1−2:1, within the experimental error of ICP, and a 1.97:1 ratio was actually found by compositional analysis in the TEM (by energy dispersive spectroscopy, EDS) of around one thousand NCs of a repeatedly cleaned sample. The drawback with repeated cleaning is that the NCs tend to aggregate; therefore this procedure was applied only to samples whose composition needed to be carefully assessed and not on those samples that underwent further cation exchange. Overall, also in this case optical absorption/emission spectra and elemental analysis proved a complete transformation of CdSe NCs to ZnSe NCs through Cu_2Se (Figure 1b). Also for these "Cu_2Se" NCs, the absorption band in the NIR region of the optical

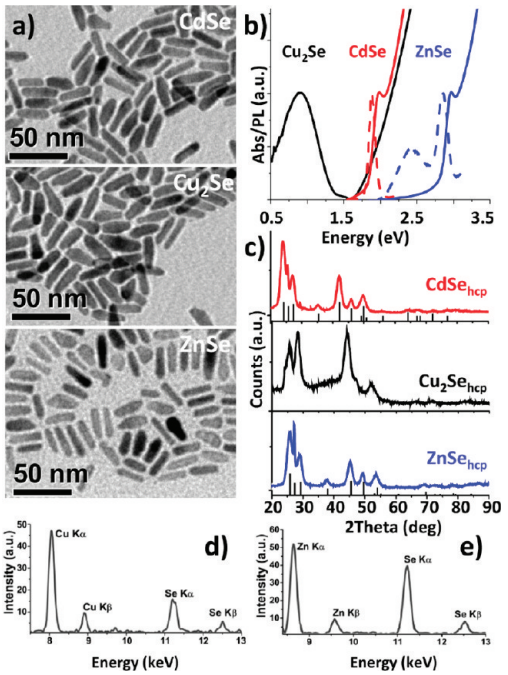

Figure 2. (a) Conventional TEM images of CdSe, Cu_2Se, and ZnSe nanorods and their corresponding (b) optical absorption/emission spectra and (c) XRD patterns. (d, e) elemental analysis via EDS of a group of Cu_2Se (d) and ZnSe (e) nanorods, which confirmed 2:1 and 1:1 stoichiometry, respectively. In the optical emission spectra of the ZnSe nanorods (blue dotted curve), the additional broad peak at around 2.5 eV is most likely due to emission from trap states.

absorption spectra might be tentatively interpreted as due to a plasmon resonance, pointing again to an actual Cu:Se stoichiometry slightly below 2:1.

The same experiments were run on various samples of spherical hcp CdSe NCs of various sizes, which always yielded spherical hcp ZnSe NCs, and by ICP analysis always Cu:Se ratios around 2.1−2:1 were found for the intermediate copper selenide NCs after repeated cleaning.[19] The compositional analysis of all these samples therefore rules out hexagonal CuSe, tetragonal umangite (Cu_3Se_2) and other phases of copper selenide with stoichiometries different from 2:1 Cu:Se as the major component. From a more detailed analysis on copper selenide nanorods (see below) we could infer that this is a metastable hcp phase of Cu_2Se.

Similar results were found indeed when converting hcp CdSe nanorods into ZnSe nanorods. Here too, the size, shape, and crystal phase of the initial nanoparticles were correctly transferred to the ZnSe NCs, i.e., hcp ZnSe nanorods were obtained at the end (Figure 2). This was also confirmed by HRTEM, and again optical absorption/emission spectra (see Figure 2d,e) indicated a full CdSe ⇒ copper selenide ⇒ ZnSe transformation. Also in this case a 2:1 Cu:Se ratio was found for the copper selenide NRs via elemental analysis by both ICP[19] and EDS;[19] however, the appearance of a plasmon band in the optical spectra suggests again a $Cu_{2-x}Se$ composition. It is interesting to note that this resonance would correspond to the transverse mode of the hole plasmon resonance for the nanorods,[33] while the longitudinal mode would fall further in the IR.

What is remarkable here too is the structure of the intermediate Cu_2Se nanorods. Also in this case the XRD patterns

dx.doi.org/10.1021/nl202927a |*Nano Lett.* 2011, 11, 4964–4970

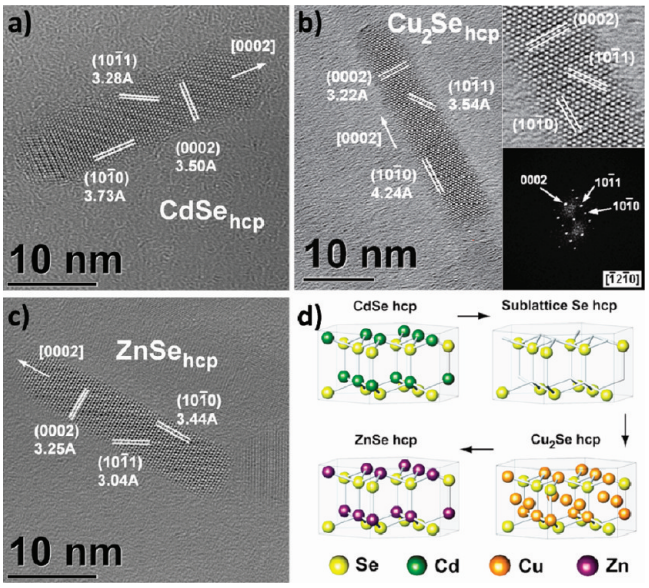

Figure 3. HRTEM images of individual (a) hcp (wurtzite) CdSe nanorods, (b) hcp Cu_2Se nanorods, and (c) hcp (wurtzite) ZnSe nanorods, where the (0 0 0 2), (1 0 −1 0) and (1 0 −1 1) lattice sets of each phase are marked; in the two insets are shown a detail of the core region of the Cu_2Se rod and its corresponding numerical electron diffraction pattern which is totally consistent with the [−1 2 −1 0] zone axis projection of hcp structure. (d) Structural sketch of hcp (0 0 0 1) slices highlighting how replacement of the cation sublattice of wurtzite CdSe, such that each Cd^{2+} ion is replaced by two Cu^+ ions, yields a chalcocite-like Cu_2Se lattice and, after the Zn cation exchange, the Cu^+ ions are removed to form a hcp ZnSe lattice.

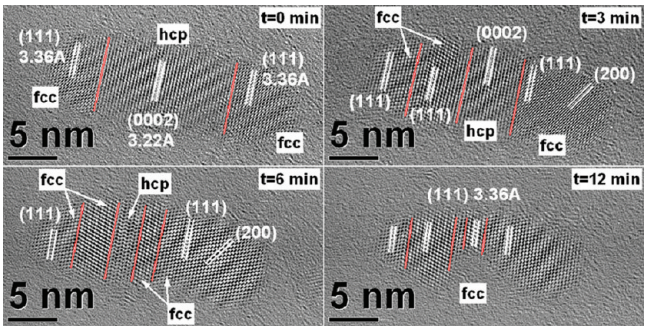

Figure 4. Beam-induced transformation of a nanorod with Cu_2Se composition and having a mixed hcp (in the central region) and fcc phase (at the tip regions). During the observation under the beam, which was carried out for 12 min, it was possible to follow the shrinkage of the central hcp region of the rod, which was progressively replaced by fcc domains, the latter expanding from the tip regions and developing a twinned texture. More details on the experiment are reported in the Supporting Information.

could not be indexed according a known phase of copper selenide. While the pattern could be partially matched with umangite (Cu_3Se_2), the presence of this phase as major component was ruled out by compositional analysis. A comparison between the XRD pattern of these Cu_2Se nanorods and the pattern of the previous spherical Cu_2Se NCs obtained from spherical hcp CdSe NCs indicated that all the diffraction peak positions matched well with each other; therefore the sample of Cu_2Se spheres and that of Cu_2Se rods appeared to have the same crystalline phase,[19] with differences in peak intensities that could be attributed to shape effects. This was also confirmed by simulations of the respective XRD patterns (see also below).

High-resolution TEM analysis of the various nanorods indicated that they all had hcp structure, including the Cu_2Se ones (Figure 3). In this case, while CdSe and ZnSe nanorods exhibited lattice spacings that were clearly compatible with the corresponding known wurtzite phases for these two materials, the Cu_2Se nanorods appeared to have a crystalline phase that is unknown in the bulk but could be described unambiguously by an hexagonal unit cell. This phase was highly unstable under the beam when the sample was observed at room temperature, and in a few seconds the structure started to convert into a fcc structure, sometimes showing a series of twinned domains in a single rod. This explains also why many fcc nanorods and a few tetragonal nanorods were additionally found in the sample by HRTEM. Longer observation times of the metastable hcp rods were possible when keeping the TEM grid at liquid nitrogen temperature, during which the hcp−fcc phase transition could be recorded easily.[19] Figure 4 reports a typical case of a rod in which the central region is hcp while the tip regions have already transformed to fcc. During the observation under the beam of this particular rod, which was carried out for 12 min, the central hcp region kept shrinking as it was progressively replaced by fcc domains expanding from the tip regions and developing a twinned texture.

From HRTEM data, acquired at low temperature, it was possible to measure the interplanar distances of this metastable hcp Cu_2Se phase and to calculate the unit cell parameters, which were $a = b = 4.96$ Å and $c = 6.42$ Å. Moreover, the corresponding numerical electron diffraction patterns in a pristine hcp rod displayed sharp diffraction spots and no additional features were present, such as streaks or satellite spots. We also carried out annealing experiments on a film of Cu_2Se nanorods under vacuum, and found (by XRD) that they converted to the cubic phase (berzelianite) at about 200 °C.[19] Interestingly, in a recent work Norris et al. also found a metastable phase in colloidal NCs, in that case for Ag_2Se NCs with tetragonal phase, which has been never reported so far for the bulk,[34] while Zheng et al. recently studied via TEM the (reversible) transient structural transformation dynamics in a single Cu_2S nanorod,[35] in that case evolving from low chalcocite to high chalcocite.

Copper selenide exists in many phases and stoichiometries,[36,37] but unlike copper sulfides and tellurides,[38] no hexagonal phase has been reported so far in the bulk for 2:1 Cu:Se stoichiometry. On the other hand, various Cu−Se clusters with Se layered structure and Cu:Se stoichiometry close to 2:1 (and up to $Cu_{140}Se_{70}$) have been synthesized by Fenske et al.[20−23] In these clusters, the arrangement of the Se layers follows a hexagonal close packing scheme and they were therefore considered by the authors as "a section of a hypothetical (up to now) unknown hexagonal modification of copper(I) selenide".[20−23] In our case, it is also interesting to note how, starting from a sphalerite CdSe lattice, replacement of Cd^{2+} ions with Cu^+ ions (twice as much), leaving the Se ion sublattice intact, yields a structure that can be identified with cubic berzelianite (or tetragonal if the lattice parameter along one direction is modified), aside from the spatial distribution of the Cu^+ ions which may occupy many sites. If the same is done with wurtzite CdSe, the corresponding structure that is obtained resembles the Cu_2S hexagonal chalcocite structure (Figure 3d). Indeed, Sadtler et al. found that wurtzite CdS nanorods convert into hexagonal chalcocite Cu_2S nanorods via cation exchange[29] and

dx.doi.org/10.1021/nl202927a |Nano Lett. 2011, 11, 4964–4970

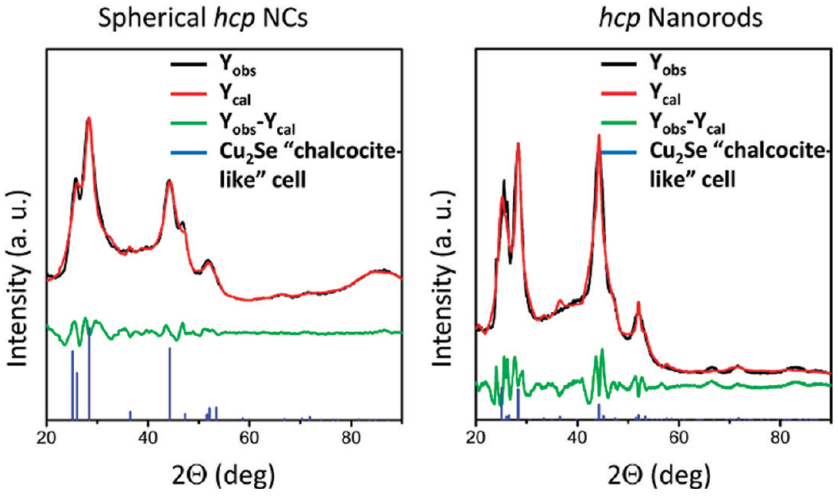

Figure 5. Whole profile fitting Rietveld-based analysis of the XRD patterns collected on both hcp spherical Cu_2Se NCs and hcp Cu_2Se nanorods, based on the hypothesis of a Cu_2Se "chalcocite-like" cell, obtained by expanding appropriately the Cu_2S cell, replacing S with Se, but keeping the same occupancies of Cu(I) species as in Cu_2S. The experimental patterns are indicated with red curves, the calculated profiles with back curves, and the residual fit profiles (experimental − calculated pattern) with green curves. The blue histograms refer to the bulk peak position for the model cells.

Luther et al. already pointed out the strong similarities in the S sublattices of Cu_2S and CdS.[11]

We performed whole profile fitting Rietveld-based analysis of the XRD patterns collected on both hcp spherical Cu_2Se NCs and hcp Cu_2Se nanorods, based on the hypothesis of a Cu_2Se "chalcocite-like" cell, obtained by expanding appropriately the Cu_2S cell, replacing S with Se, but keeping the same occupancies of Cu(I) species as in Cu_2S. We used a whole profile fitting Rietveld-based program, named FullProf, and took into account crystal structure models, instrumental broadening contributions, and possible shape anisotropies.[39] A summary of this analysis is reported here, while additional details are discussed in the Supporting Information.[19] The results of the fits are shown in Figure 5, which reports both the experimental pattern (red curve) and the Rietveld best calculated profile (black curve) for the two samples. Residual fit profiles (experimental − calculated pattern) are also shown (green curve).

The following conclusions could be drawn from the fits: (i) For the spherical Cu_2Se NCs obtained from spherical wurtzite CdSe NCs, the hypothesis of an hexagonal intermediate Cu_2Se phase, obtained by the structure of high chalcocite Cu_2S upon replacement of the S atomic species with Se, was found to explain the measured patterns. Refined parameters were the unit cell size ($a_{refined}$ = 4.09 Å and $c_{refined}$ = 6.86 Å) and the *B* factors of the Cu atoms. The latter were found to reach quite high values, which is indicative of an important lattice disorder for those ions. (ii) Also for the case of rodlike hcp NCs the hypothesis of an hexagonal "chalcocite-like" intermediate Cu_2Se phase was found to reproduce the experimental pattern. Refined parameters were the *B* factors of the Cu atoms and the unit cell size ($a_{refined}$ = 4.09 Å and $c_{refined}$ = 20.49 Å). The unit cell found in this second case is just a multiple of the previous unit cell along the *c* axis. Indeed the two refined cells have the same cell parameter *a*, while in the second cell the parameter along the *c* axis is simply a multiple (3×) of the corresponding parameter of the previous cell. In fitting the pattern of the rod sample, we additionally took into account the anisotropic peak broadening due to the elongated shape. It is important to stress here that the Rietveld analysis of the Cu_2Se hcp NCs, both for spherical and rodlike shape, gave us a possible and reasonable structural solution, which however does not rule out other possible solutions. On the other hand, HRTEM analysis showed that we are in the presence of NCs crystallized in a phase that can be uniquely described by a hexagonal cell.

It is interesting to compare interatomic distances between Se atoms in this "chalcocite-like" cell with the corresponding distances in the copper selenide clusters of Fenske et al. where the Se layers are stacked in a ABA hexagonal close packing sequence.[22] In the present cell, interlayer distances between Se atoms are around 4.16 Å, while for example in Fenske's cluster named as "Compound 1" in ref 22 they ranged from 3.6 to 4.8 Å. Distances between Se atoms in the same layer in the present cell are equal to 4.09 Å (that is, the *a* lattice parameter), while in Fenske's clusters they ranged from 3.55 to 4.57 Å, with average distance equal to 4.21 Å.

For the Cu_2Se NCs obtained by cation exchange from wurtzite CdSe NCs to be in a more energetically stable lattice than the hcp one, such as cubic or tetragonal, cation exchange of Cd^{2+} with Cu^+ must also be accompanied by slip of the Se layers from hexagonal close packing to cubic close packing, which apparently requires an activation energy. This appears to be provided by thermal annealing or, alternatively, by the energetic electron beam in the TEM microscope. Even more interesting, since the following $Cu^+ \rightleftharpoons Zn^{2+}$ reaction on these NCs is carried out at temperatures up to 250 °C, at which the nanocrystals should have converted to a more stable phase (cubic/tetragonal), we conclude that in the liquid medium the process of exchange of Cu^+ with Zn^{2+} occurs at a much faster rate than the phase transition of the hcp phase to berzelianite/tetragonal $Cu_{2-x}Se$, which allows the hexagonal symmetry of the anionic lattice to be safely transferred from Cu_2Se to ZnSe.

One important aspect of the reactions discussed in this work is related to the driving force of the cation exchange. In many of the various cation exchange reactions in nanoscale materials that have been studied so far[7,14,29,40−50] the driving force appeared to be related to the higher stability of the compound formed upon exchange. This applies for example to the transformations of CdSe to Ag_2Se[7] and of CdSe to $Cu_{2-x}Se$ NCs (in the latter case for instance Cu^+ has a much greater affinity for Se than Cd^{2+}). In

dx.doi.org/10.1021/nl202927a |*Nano Lett.* 2011, 11, 4964–4970

other cases, the introduction of complexing agents for the cation that is extracted from the lattice can provide an additional driving force which can affect significantly the course of a given reaction.[11] To cite a few examples, oleylamine promoted the cation exchange from SnSe to PbSe NCs[42] and didodecyldimethylammonium bromide provided the metal salts solubility and then accelerated the cation exchange reaction from CdE to M_xE_y NCs (E = S, Se, Te; M = Pd, Pt).[41] However, to the best of our knowledge, cation exchange from copper selenide to zinc selenide had remained an unsolved problem so far. The reason is most likely that the chemical bond between Cu and Se is much stronger than that between Zn and Se. Our group reported a cation exchange procedure from $Cu_{2-x}Se$ to CdSe,[13] but those conditions, when tested in the $Cu_{2-x}Se$ to ZnSe exchange step (except for replacing a Cd^{2+} salt, either oleate or phosphonate, with the corresponding Zn^{2+} salt), were unsuccessful.

Herein, three key aspects contributed to the success of cation exchange reaction from copper selenide to zinc selenide: first, the zinc ion solution was prepared by dissolving zinc chloride in oleylamine. The bonding between zinc ions and oleylamine is much weaker than that involved in zinc oleate and zinc phosphonate;[51] therefore zinc ions, while still being well dispersed in solution, are readily available for the reaction. Second, TOP, as a soft base, binds more strongly to the Cu^+ cation (which is a soft acid) than to Zn^{2+}, since phosphorus is one of the best soft donor atoms for Cu(I) so it is a good complexing agent for the extracted Cu^+ ions,[52] which should make the overall reaction thermodynamically favored. The use of phosphine as a soft base to bind to Cu^+ and favor cation exchange was already reported in previous works.[7,11,29,41] Third, the reaction is preformed at 250 °C instead of room temperature, which should favorably affect the diffusion of the cation species inside the nanocrystal lattice. Furthermore, well-dispersed ZnSe NCs are obtained at high temperature, since better surface passivation is achieved in this case by the various ligands present in solution. Indeed, our attempt to perform the same reaction at room temperature in a mixture of toluene and methanol was not successful, as only partially exchanged and aggregated particles were obtained in that case. Furthermore, this reaction might also be favored entropically, since for every Zn^{2+} ion that enters the lattice two Cu^+ ions are released (and obviously the free ions in solution will have higher entropy than the ones bound in the lattice). The contribution from the entropic term will additionally increase at the high temperature at which the exchange is carried out.

Another important aspect is connected with the phase stability of the hcp ZnSe NCs that we obtained by cation exchange. Annealing experiments carried out in situ in the TEM on ZnSe nanorods (from 25 °C) up to 650 °C did not modify their structure, which remained hcp.[19] We also recorded XRD spectra on samples of ZnSe nanorods kept under vacuum at temperatures up to 900 °C (melting point of bulk ZnSe is 1525 °C) and they remained in the wurtzite phase. These findings are certainly interesting, given that the most stable phase for them should be fcc, and require further investigation.

In conclusion, we have shown that colloidal copper selenide NCs represent versatile intermediates for accessing ZnSe NCs by cation exchange from CdSe NCs: First, fcc/tetragonal $Cu_{2-x}Se$ NCs can be obtained from cubic sphalerite CdSe NCs by replacing Cd^{2+} with Cu^+ ions. From them, cubic sphalerite ZnSe NCs can be prepared by replacing Cu^+ with Zn^{2+} ions. It is also possible to exchange Cd^{2+} with Cu^+ in hexagonal wurtzite CdSe NCs, which yields Cu_2Se NCs in a metastable hexagonal phase and from them wurtzite ZnSe NCs are obtained by exchanging Cu^+ with Zn^{2+}. All these transformations preserve both size and shape of the starting nanostructures. Colloidal NCs in metastable crystal phases might be exploited also in other materials systems for fabricating nanostructures in phases that are not easily accessible by direct chemical synthesis.

■ ASSOCIATED CONTENT

Supporting Information. Additional data on chemicals and synthesis procedures, optical and XRD characterization, TEM and STEM analysis, elemental analysis, XRD analysis, and estimate of size distributions. This material is available free of charge via the Internet at http://pubs.acs.org.

■ AUTHOR INFORMATION

Corresponding Author
*E-mail: liberato.manna@iit.it.

■ ACKNOWLEDGMENT

This work was financially supported in part by the FP7 starting ERC Grant NANO-ARCH (Contract No. 240111) and by IIT SEED Grant XMI-LAB, IIT no. 21537. We thank Dirk Dorfs (IIT Genova) and Kunlun Ding (University of California, Santa Barbara) for many useful discussions.

■ REFERENCES

(1) Mokari, T. *Nano Rev.* **2011**, *2*, 5983.
(2) Talapin, D. V.; Lee, J. S.; Kovalenko, M. V.; Shevchenko, E. V. *Chem. Rev.* **2010**, *110*, 389.
(3) Carbone, L.; Cozzoli, P. D. *Nano Today* **2010**, *5*, 449.
(4) Costi, R.; Saunders, A. E.; Banin, U. *Angew. Chem., Int. Ed.* **2010**, *49*, 4878.
(5) Lo, S. S.; Mirkovic, T.; Chuang, C. H.; Burda, C.; Scholes, G. D. *Adv. Mater.* **2011**, *23*, 180.
(6) Donega, C. D. M. *Chem. Soc. Rev.* **2011**, *40*, 1512.
(7) Son, D. H.; Hughes, S. M.; Yin, Y. D.; Alivisatos, A. P. *Science* **2004**, *306*, 1009.
(8) Robinson, R. D.; Sadtler, B.; Demchenko, D. O.; Erdonmez, C. K.; Wang, L. W.; Alivisatos, A. P. *Science* **2007**, *317*, 355.
(9) Jain, P. K.; Amirav, L.; Aloni, S.; Alivisatos, A. P. *J. Am. Chem. Soc.* **2010**, *132*, 9997.
(10) Li, J. S.; Zhang, T. R.; Ge, H. P.; Yin, Y. D.; Zhong, W. W. *Angew. Chem., Int. Ed.* **2009**, *48*, 1588.
(11) Luther, J. M.; Zheng, H. M.; Sadtler, B.; Alivisatos, A. P. *J. Am. Chem. Soc.* **2009**, *131*, 16851.
(12) Deka, S.; Genovese, A.; Zhang, Y.; Miszta, K.; Bertoni, G.; Krahne, R.; Giannini, C.; Manna, L. *J. Am. Chem. Soc.* **2010**, *132*, 8912.
(13) Deka, S.; Miszta, K.; Dorfs, D.; Genovese, A.; Bertoni, G.; Manna, L. *Nano Lett.* **2010**, *10*, 3770.
(14) Pietryga, J. M.; Werder, D. J.; Williams, D. J.; Casson, J. L.; Schaller, R. D.; Klimov, V. I.; Hollingsworth, J. A. *J. Am. Chem. Soc.* **2008**, *130*, 4879.
(15) Dabbousi, B. O.; RodriguezViejo, J.; Mikulec, F. V.; Heine, J. R.; Mattoussi, H.; Ober, R.; Jensen, K. F.; Bawendi, M. G. *J. Phys. Chem. B* **1997**, *101*, 9463.
(16) Kudera, S.; Zanella, M.; Giannini, C.; Rizzo, A.; Li, Y. Q.; Gigli, G.; Cingolani, R.; Ciccarella, G.; Spahl, W.; Parak, W. J.; Manna, L. *Adv. Mater.* **2007**, *19*, 548.
(17) Reiss, P.; Bleuse, J.; Pron, A. *Nano Lett.* **2002**, *2*, 781.
(18) Sung, Y. M.; Park, K. S.; Lee, Y. J.; Kim, T. G. *J. Phys. Chem. C* **2007**, *111*, 1239.

(19) Additional details on materials and methods are available in the Supporting Information.
(20) Dehnen, S.; Fenske, D. *Angew. Chem., Int. Ed.* **1994**, *33*, 2287.
(21) Zhu, N. Y.; Fenske, D. *J. Chem. Soc., Dalton Trans.* **1999**, 1067.
(22) Fu, M. L.; Issac, I.; Fenske, D.; Fuhr, O. *Angew. Chem., Int. Ed.* **2009**, *49*, 6899.
(23) Corrigan, J. F.; Fuhr, O.; Fenske, D. *Adv. Mater.* **2009**, *21*, 1867.
(24) Reiss, P. *New J. Chem.* **2007**, *31*, 1843.
(25) Yeh, C.-Y.; Lu, Z. W.; Froyen, S.; Zunger, A. *Phys. Rev. B* **1992**, *46*, 10086.
(26) Kumar, P.; Singh, K. *J. Optoelectron. Biomed. Mater.* **2009**, *1*, 59.
(27) Xi, B. J.; Xiong, S. L.; Xu, D. C.; Li, J. F.; Zhou, H. Y.; Pan, J.; Li, J. Y.; Qian, Y. T. *Chem.—Eur. J.* **2008**, *14*, 9786.
(28) Liu, S. Y.; Choy, W. C. H.; Jin, L.; Leung, Y. P.; Zheng, G. P.; Wang, J. B.; Soh, A. K. *J. Phys. Chem. C* **2007**, *111*, 9055.
(29) Sadtler, B.; Demchenko, D. O.; Zheng, H.; Hughes, S. M.; Merkle, M. G.; Dahmen, U.; Wang, L. W.; Alivisatos, A. P. *J. Am. Chem. Soc.* **2009**, *131*, 5285.
(30) De Montreuil, L. *Econ. Geol.* **1975**, *70*, 384.
(31) Kogut, A. N.; Mel'nik, A. I.; Mikolaichuk, A. G.; Romanishin, B. M. *Russ. Phys. J.* **1973**, *16*, 1113.
(32) Dorfs, D.; Härtling, T.; Miszta, K.; Bigall, N. C.; Kim, M. R.; Genovese, A.; Falqui, A.; Povia, M.; Manna, L. *J. Am. Chem. Soc.* **2011**, *133*, 11175.
(33) Krahne, R.; Morello, G.; Figuerola, A.; George, C.; Deka, S.; Manna, L. *Phys. Rep* **2011**, *501*, 75.
(34) Sahu, A.; Qi, L. J.; Kang, M. S.; Deng, D.; Norris, D. J. *J. Am. Chem. Soc.* **2011**, *133*, 6509.
(35) Zheng, H. M.; Rivest, J. B.; Miller, T. A.; Sadtler, B.; Lindenberg, A.; Toney, M. F.; Wang, L. W.; Kisielowski, C.; Alivisatos, A. P. *Science* **2011**, *330*, 206.
(36) Heyding, R. D.; Murray, R. M. *Can. J. Chem.* **1976**, *54*, 841.
(37) Zheng, X. W.; Hu, Q. T. *Appl. Phys. A: Mater. Sci. Process.* **2009**, *94*, 805.
(38) El-Barhawi, M. S.; Khodier, S.; Kishk, S. S.; Nagib, N. N. *Appl. Phys. A: Mater. Sci. Process.* **1994**, *58*, 601.
(39) Fullprof http://www-llb.cea.fr/fullweb/.
(40) Miszta, K.; Dorfs, D.; Genovese, A.; Kim, M. R.; Manna, L. *ACS Nano* DOI:10.1021/nn201988w.
(41) Wark, S. E.; Hsia, C. H.; Son, D. H. *J. Am. Chem. Soc.* **2008**, *130*, 9550.
(42) Kovalenko, M. V.; Talapin, D. V.; Loi, M. A.; Cordella, F.; Hesser, G.; Bodnarchuk, M. I.; Heiss, W. *Angew. Chem., Int. Ed.* **2008**, *47*, 3029.
(43) Smith, A. M.; Nie, S. *J. Am. Chem. Soc.* **2010**, *133*, 24.
(44) Taniguchi, S.; Green, M.; Lim, T. *J. Am. Chem. Soc.* **2011**, *133*, 3328.
(45) Rivest, J. B.; Swisher, S. L.; Fong, L.-K.; Zheng, H.; Alivisatos, A. P. *ACS Nano* **2011**, *5*, 3811.
(46) Camargo, P. H. C.; Lee, Y. H.; Jeong, U.; Zou, Z.; Xia, Y. *Langmuir* **2007**, *23*, 2985.
(47) Zhong, X. H.; Feng, Y. Y.; Zhang, Y. L.; Gu, Z. Y.; L., Z. *Nanotechnology* **2007**, *18*, 385606.
(48) Lambert, K.; De Geyter, B.; Moreels, I.; Hens, Z. *Chem. Mater.* **2009**, *21*, 778.
(49) Moon, G. D.; Ko, S. W.; Xia, Y.; Jeong, U. Y. *ACS Nano* **2010**, *4*, 2307.
(50) Ethayaraja, M.; Bandyopadhyaya, R. *Ind. Eng. Chem. Res.* **2008**, *47*, 5982.
(51) Li, L. S.; Pradhan, N.; Wang, Y.; Peng, X. *Nano Lett.* **2004**, *4*, 2261.
(52) *Encyclopedia of Inorganic Chemistry*, 2nd ed.; King, R. B., Ed.; Wiley: Chichester and New York, 2005.